

CHAPTER 112

BED RESPONSE TO FAIRWEATHER AND STORM FLOW ON THE SHOREFACE

Malcolm O. Green¹, John D. Boon², Jeffrey H. List²
and L. Don Wright²

Abstract

Bailard's (1981) model of combined-flow, total-load sediment transport was used to calculate sediment flux at 8-m depth on a wave-dominated shoreface during fairweather and during a storm. Waves were skewed onshore during fairweather, however it was the reversing tidal current that controlled predicted transport direction. Transport direction during the early phase of the storm was also controlled by the mean flow, this time a wind-driven jet-like flow with an offshore component. As the storm progressed, waves became more organized and highly skewed, and by the end of the storm, predicted sediment transport was turned onshore by the shoreward-skewed waves against the mean flow. Measurements of changes in relative bed elevation at the 8-m depth site were used to verify the transport predictions. A total of 6 cm of accretion occurred over 4.5 days of low-energy flow. It was found that predicted onshore transport was strongly correlated with erosion at the 8-m depth site, and predicted offshore transport was strongly correlated with accretion. Five cm of scour occurred during the initial phase of the storm, followed by 15 cm of rapid accretion. Onset of accretion was coincident with the organization of surface waves into long-period swell, and the maximum accretion rate was coincident with the most highly-skewed waves.

¹Department of Earth Sciences, University of Cambridge, Downing Street, Cambridge, CB2 3EQ, United Kingdom.

²Virginia Institute of Marine Science, School of Marine Science, College of William and Mary, Gloucester Point, VA 23062, U.S.A.

Introduction

Direct measurement of sediment transport by combined wave and current flow has not kept pace with measurement of the velocity fields that drive transport. Consequently, although the properties of the velocity field that are theoretically germane to sediment transport are generally recognized, and in some cases well understood, models that link bed response to flow properties remain largely untested.

Properties of the combined flow relevant to sediment transport include, in one form or another, the mean, variance, and skewness. The mean flow advects sediment suspended in the water column; the variance is a measure of the kinetic energy available for entraining sediment from the bed; and velocity skewness translates into net transport of that component of the sediment load that fluctuates with the instantaneous velocity. Rigorous extensions of Bagnold's (1963) unidirectional transport model by Bowen (1980) and Bailard (1981) have given specific form to the relevant flow properties and subsequently stimulated much research. Bailard (1981) gave the following equation for total-load (sum of bedload and suspended load) time-averaged sediment transport:

$$\begin{aligned} \langle i_t \rangle = & (\rho C_f c_b / \tan \phi) [\langle U_t^3 \rangle + (\tan \beta / \tan \phi) \langle |U_t|^3 \hat{i} \rangle] \\ & + (\rho C_f c_s / w) [\langle |U_t|^3 U_t \rangle + (-s \tan \beta / w) \langle |U_t|^5 \hat{i} \rangle] \dots (1) \end{aligned}$$

where U_t is the instantaneous velocity, β is the local bed slope, ϕ is the coefficient of internal friction of the bed, w is the sediment settling velocity, ρ is the fluid density, C_f is a drag coefficient, c_b and c_s are the suspended-load and bedload efficiencies respectively, and $\langle i_t \rangle$ is an immersed-weight transport rate (units of weight per time per unit width, i.e. mass/time³). The angle brackets denote time-averaging, and boldface characters indicate vector quantities. \hat{i} is the unit vector in the cross-slope direction, positive downslope, and for the purposes of the following analysis, the unit vector \hat{i} also corresponds to the shore-normal direction (positive offshore).

The two terms in equation (1) that involve time-averages of odd or signed powers of the instantaneous velocity, i.e. $\langle U_t^3 \rangle$ in the bedload term and $\langle |U_t|^3 U_t \rangle$ in the suspended-load term, reflect the skewness of the velocity distribution and denote the bedload and suspended-load fluxes that are driven by and parallel to the instantaneous velocity. Both terms are identically zero for a symmetrical, zero-mean velocity distribution. The

two terms that involve time-averages of powers of absolute values of the instantaneous velocity, i.e. $\langle |U_t|^3 \rangle$ in the bedload term and $\langle |U_t|^5 \rangle$ in the suspended-load term, reflect the flow energy and are considered to govern the bedload and suspended-load fluxes that fall downhill under the influence of gravity. Unlike the former terms, both of these terms are non-zero for a symmetrical, zero-mean velocity distribution.

Guza and Thornton (1985) decomposed the total velocity into mean ($\bar{}$) and oscillatory ($\tilde{}$) components:

$$U_t = (\tilde{u} + \bar{u})\hat{i} + (\tilde{v} + \bar{v})\hat{j} \dots\dots\dots(2)$$

where \hat{j} is the unit vector in the alongslope direction, and showed how each component theoretically contributes to each of the terms in the transport equation. The terms involving velocities in equation (1) are frequently referred to as "velocity moments" although this is technically inaccurate, firstly because they are not dimensionless, and secondly, and more importantly, because they are not computed from a zero-mean velocity distribution. The mean flow skews the velocity distribution and adds kinetic energy; the mean flow cannot be presumed a priori to be subordinate, in terms of sediment transport, to the oscillating component of the total velocity.

The objective of this paper is to test the theoretical links between the properties of the velocity distribution and sediment transport as expressed in equation (1). The data set, obtained from 8-m depth on a wave-dominated, microtidal shoreface, consists of simultaneous measurements of near-bed velocities and changes in relative bed elevation at a single point. Sediment flux thus was not measured directly, however the record of local sedimentation is useful for the stated objective if it is viewed as the product, and therefore the close analog, of sediment transport.

Observed velocity distributions are described, and the contributions made by the mean flow and oscillating flow to each of the velocity "moments" in the transport equation are compared. Equation (1) is used to calculate sediment transport, and the transport predictions are tested by seeking purely qualitative correlations between terms in the transport equation and observed changes in relative bed elevation.

Methods

Observations were made over a period of 8 days from 6 to 14 September, 1985, at 8-m depth on the shoreface that fronts the barrier-island coast at Duck, North Carolina, on the U.S. Atlantic coast (Figure 1). The experiment was one

component of a larger nearshore processes experiment, DUCK85, which was conducted at the U.S. Army Corps of Engineers' Field Research Facility; details of the DUCK85 experiment can be found in Mason et al. (1987).

Currents were measured at 20 cm above the bed with a 4.0-cm diameter Marsh-McBirney electromagnetic current meter supported on a bottom-mounted tripod and controlled by a Sea-Data Model 635-9RS logger. Currents were sampled at 1 s intervals for 2048 s every 2 hours. Relative bed elevation was measured using a Datasonics Model ASA-920 digital sonar altimeter (DSA) mounted 4 m from the main tripod on a platform supported by pipes driven 50 cm into the seabed. The DSA is a high-resolution (0.15 cm) sonar device that converts reflected travel time of a high-frequency (1 MHz) acoustic pulse into a digital number that is proportional to the distance between the transducer and the seabed. Green and Boon (1988) described the calibration of the unit, its zero stability, and its performance over a rippled bed and when suspended sediment concentration is high, and concluded that the altimeter performed reliably and predictably in the field. The DSA was polled every 8 s by the Sea-Data logger, for a total of 256 observations per 2048-s burst.

Green (1987), drawing from bathymetric and side-scan sonar data, demonstrated that the Duck shoreface exhibits scant longshore variability, and is well represented by a simple two-dimensional concave-upwards profile. If it is assumed that sediment transport along the straight and parallel contours of the Duck shoreface is uniform, then it is the cross-shore component of the instantaneous velocity that controls erosion and sedimentation seaward of the surfzone. Thus, the longshore component of velocity can be neglected; for the purposes of the following analysis it is assumed that $U_t = (\bar{u} + \bar{u}')\hat{i}$, and all sediment fluxes are thus cross-shore fluxes.

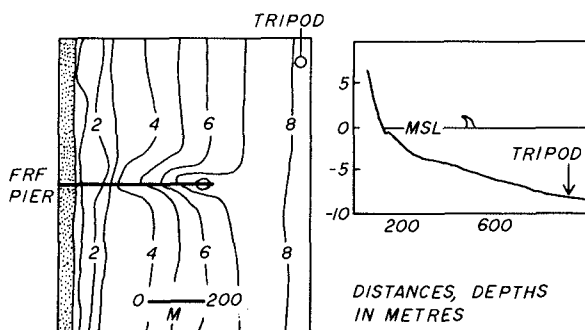


Figure 1. Experiments were conducted at 8-m depth seaward of the surfzone. The Field Research Facility (FRF) is situated in the southern Mid-Atlantic Bight, between Cape Hatteras to the south and Chesapeake Bay to the north. Bathymetry based on surveys by personnel of the FRF.

Predicted Sediment Transport

During the first 4.5 days of the deployment, waves were low (<60 cm) and long (10 s) and the wind light (<6 m/s) and directed offshore. A shift of the wind to the northeast (onshore) at 0700 hours on September 11 signalled the end of fairweather conditions; for the next 3.5 days, the wind blew from the northeast at speeds generally in excess of 10 m/s. See Wright et al. (1986) for a detailed description of the evolution of the storm.

Prior to the storm, the burst standard deviation of the cross-shore component of velocity measured at $z = 20$ cm averaged 10 cm/s (Figure 2), and most of the variance was due to surface gravity waves: infragravity band (0.01 to 0.05 Hz) energy in the velocity record was two orders of magnitude smaller than energy in the incident band (0.05 to 0.5 Hz). The burst-averaged cross-shore current attained maximum speeds of -5 cm/s, and the sign of \bar{u} reversed at approximately the semi-diurnal frequency (Figure 2), indicating a strong contribution by the astronomical tide.

Current energy in the incident and infragravity bands increased through the storm at approximately equal rates. The burst standard deviation of the cross-shore velocity reached a peak of nearly 40 cm/s 2.2 days after the windshift (Figure 2), at which time the significant wave height was 2.10 m and individual maxima in the cross-shore velocity exceeded 150 cm/s. The mean flow during the storm resembled a jet-like coastal flow, (Wright et al., 1986), setting alongshore to the south at an average of 33 cm/s and offshore at a maximum of 10 cm/s.

Those terms in equation (1) that denote sediment flux parallel to the instantaneous velocity are governed themselves by both the mean and skewness of the velocity distribution. Shown in Figure 3 are observed values of

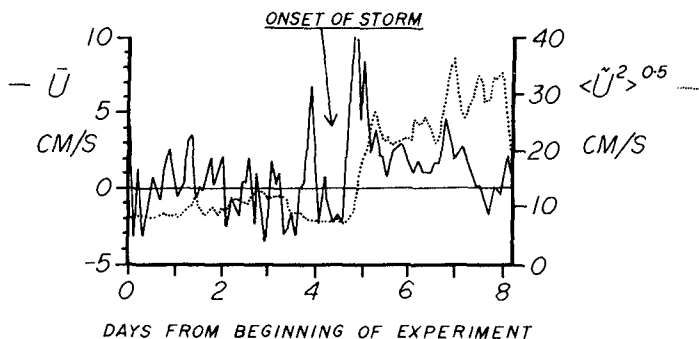


Figure 2. Burst mean cross-shore current speed (\bar{u}) and burst standard deviation of the cross-shore component of velocity ($\langle \tilde{u}^2 \rangle^{0.5}$), both measured at $z = 20$ cm, 8-m depth. The onset of the northeaster storm is indicated.

$\langle \tilde{u}^3 \rangle$, which reflects the wave-orbital velocity asymmetry only since the mean flow is removed; and $\langle U_t^3 \rangle$, which reflects the asymmetry of the total flow. The averaging period corresponds to the burst duration. Observed values of $\langle u^3 \rangle$ were negative throughout the fairweather period, which indicates a higher than Gaussian occurrence of large negative (i.e. onshore) velocities and which is consistent with the expectation from theory of relatively long (10 s) waves in relatively shallow water (~10 m) being skewed in the direction of propagation. In contrast, during the early stages of the storm there was no consistent sign to the wave skewness, which reflects the stage of developing wind-waves at that time with surface waves driven locally before the strong northeast wind. Approximately 1.3 days after the onset of the storm, $\langle \tilde{u}^3 \rangle$ again became consistently negative, and thereafter increased in magnitude. Towards the end of the experiment, 3.5 days from the onset of the storm, $\langle \tilde{u}^3 \rangle$ attained its largest negative value, reflecting the marked asymmetry of the organized long-period and large-amplitude swell that was the legacy of the storm.

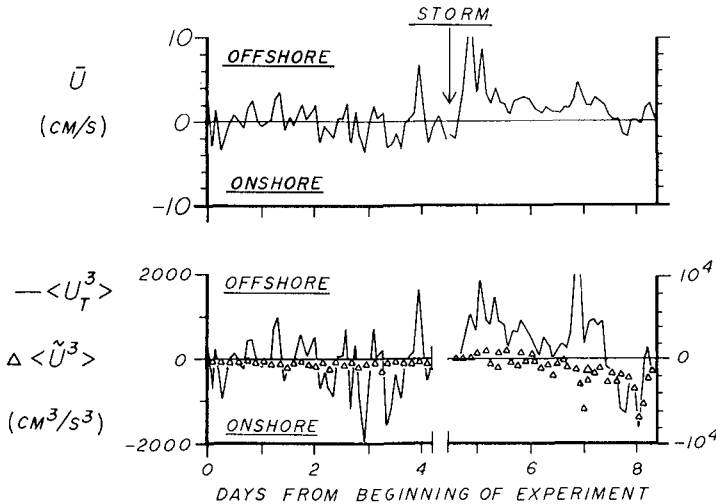


Figure 3. Wave-orbital velocity skewness, $\langle \tilde{u}^3 \rangle$, and total velocity skewness, $\langle U_t^3 \rangle$, measured at the 8-m depth site, $z = 20$ cm. Horizontal axis is time in days from the beginning of the experiment; note the break of scale at 4.5 days which corresponds to the onset of the storm. The vertical scale on the left refers to the fairweather period, and the vertical scale on the right to the storm period. Also shown is the mean cross-shore current speed flow at $z = 20$ cm.

The oscillatory velocities, however, did not usually make the major contribution to the skewness of the total flow. Except at the end of the storm, when wave-orbital velocities were most highly skewed, the sign of the total-flow skewness (i.e. $\langle U_t^3 \rangle$) was the same as the sign of the mean cross-shore flow, regardless of the wave asymmetry (Figure 3). Thus, the skewness of the observed velocity distributions was controlled by the tidal mean flow during fairweather, by the wind-driven mean flow for much of the storm, and by the oscillatory component of the total flow only towards the end of the storm. The higher-order signed velocity moment that appears in the suspended-flux term (i.e. $\langle |U_t|^3 U_t \rangle$) behaved in essentially the same fashion as the lower-order moment, and need not be examined further here.

In contrast, the mean flow was less important to those velocity terms that reflect the kinetic energy of the flow and that govern the downhill sediment flux. The third-order zero-mean term, $\langle |\tilde{u}|^3 \rangle$, averaged $1.56 \langle \tilde{u}^2 \rangle^{3/2}$ and $1.59 \langle u^2 \rangle^{3/2}$ over the fairweather and storm periods respectively, where the theoretical value is $1.20 \langle \tilde{u}^2 \rangle^{3/2}$ assuming a monochromatic sea and $1.60 \langle \tilde{u}^2 \rangle^{3/2}$ assuming a linear random sea (Guza and Thornton, 1985). The fifth-order zero-mean term, $\langle |\tilde{u}|^5 \rangle$, averaged $5.76 \langle \tilde{u}^2 \rangle^{5/2}$ and $6.26 \langle u^2 \rangle^{5/2}$ over the same periods, where the theoretical value is $1.92 \langle \tilde{u}^2 \rangle^{5/2}$ and $6.38 \langle \tilde{u}^2 \rangle^{5/2}$ assuming monochromatic and linear random seas respectively. Over the fairweather period, the mean flow increased the value of the third-order zero-mean term by 8% on average (i.e. $\langle |U_t|^3 \rangle / \langle |\tilde{u}|^3 \rangle = 1.08$) and the fifth-order zero-mean term by 13% on average. During the storm, 10% and 19% on average were added to the third- and fifth-order zero-mean terms respectively by the mean flow.

Sediment flux at the 8-m depth site was predicted from the velocity data using equation (1) and averaging over the burst length (34 minutes). The predicted burst-averaged bedload flux, suspended-load flux, and total-load flux are shown in Figure 4 for both the fairweather and storm periods. All fluxes are cross-shore components and the following constants were assumed: $C_f = 0.003$ (Sternberg, 1972), adjusted to apply to the velocity at $z = 20\text{cm}$; $\epsilon_b = 0.21$, $\epsilon_s = 0.025$ (Baillard, 1981); $w = 1.5\text{ cm/s}$ (determined in the laboratory); $\tan \phi = 0.63$ (Guza and Thornton, 1985); and $\tan \beta = 0.0055$ (measured).

During the fairweather period, the bedload and suspended-load components of the predicted total load were approximately equal in magnitude, while during the storm, suspended load accounted for approximately three-quarters

of the predicted total load (Figure 4). Since the factor $\rho C_f c_b / \tan \phi$ is three orders of magnitude greater than the factor $\rho C_f c_b \tan \beta / \tan^2 \phi$, for the gravity component of the bedload flux to be comparable in magnitude to the velocity-driven component, the total velocity must be both energetic ($\langle |U_t|^3 \rangle$ large) and nearly symmetrical about zero ($\langle U_t^3 \rangle$ small), which was generally never the case in either fairweather or storm conditions. Similarly, $\rho C_f c_s / w$ is four orders of magnitude greater than $\rho C_f c_s^2 \tan \beta / w^2$, and thus the gravity component of the suspended-load flux was subordinate to the velocity-driven component. Thus, during fairweather, since the mean flow controlled the total-flow skewness and the sediment flux was predominantly driven by the instantaneous velocity, the cross-shore components of the predicted bedload and suspended-load fluxes reversed sign in phase with the mean (tidal) flow (Figure 4). During the early stage of the storm, when the total-flow skewness was controlled by the wind-driven mean flow, predicted net sediment flux was directed offshore, and during the later stage of the storm, when the total-flow skewness was controlled by the wave asymmetry, predicted sediment flux was directed onshore (Figure 4).

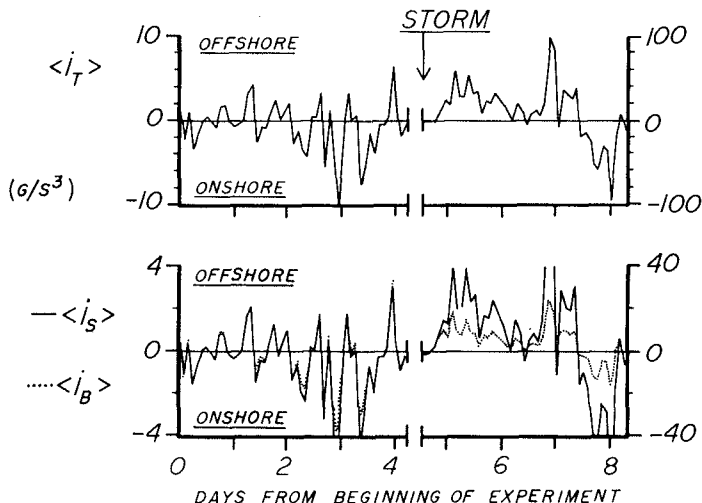


Figure 4. Predicted cross-shore total-load, suspended-load and bedload sediment flux at the 8-m depth site. The horizontal axis is time in days from the beginning of the experiment; note the break of scale at 4.5 days which corresponds to the onset of the storm. The vertical scale on the left refers to the fairweather period, and the vertical scale on the right to the storm period.

Observed Bed Response to Fairweather and Storm Flow

Fairweather

The DSA record was burst-averaged after all wild points in the data were removed. Generally, during low-energy conditions, the DSA signal was quite flat, however, when spikes did occur, they were easily recognized and removed. Green and Boon (1988) provide a discussion of the editing procedure, and show actual time-series of instantaneous relative bed elevation.

In a series of laboratory tests, Green and Boon (1988) also demonstrated that the sonic beamwidth was finite, and that positioning the instrument at a height above the bed greater than eight times the height of the wave ripples guaranteed that only the tops of the wave ripples were sensed. Since bedforms at the 8-m depth site were symmetrical wave ripples 3 cm high by 15 cm long, and the DSA was located approximately 50 cm above the bed, the DSA record should therefore not be confounded by the local topography.

The burst-averaged relative bed elevation over the fairweather segment of the experiment, expressed as cm below the fixed elevation of the transducer, is shown in Figure 5. Over the 4.5 days of low-energy preceding the storm, a total decrease in relative bed elevation of nearly 6 cm was recorded. Assuming the absolute elevation of the DSA is fixed, three points substantiate the conclusion that the observed change in relative bed elevation represents accretion at the 8-m depth site: divers observed no local bed disturbances induced by the instrument; migrating wave ripples (3 cm high by 15 cm long) could not have caused the observed signal; and the zero drift of the DSA was negligible (Green and Boon, 1988).

Green (1987) applied a combined-flow boundary-layer model to the fairweather velocity data and showed that the combined-flow skin friction at 8-m depth exceeded that necessary to initiate sediment transport for almost the entire fairweather period. Green also modelled the sediment-flux divergence associated with the competent fairweather combined wave and current flow, and showed that the cross-shore distribution of sediment sinks and sources on the shoreface associated with onshore transport differed fundamentally from that associated with offshore transport. At 8-m depth, erosion was predicted to occur under net onshore transport during fairweather, and accretion was predicted to occur under net offshore transport. Thus, if the observed change in relative bed elevation during times of predicted onshore transport differs consistently from that observed during times of predicted offshore transport, then this would be at least qualitative verification of the transport predictions provided by equation (1).

Inspection of the DSA record in Figure 5 reveals a connection between predicted transport direction and

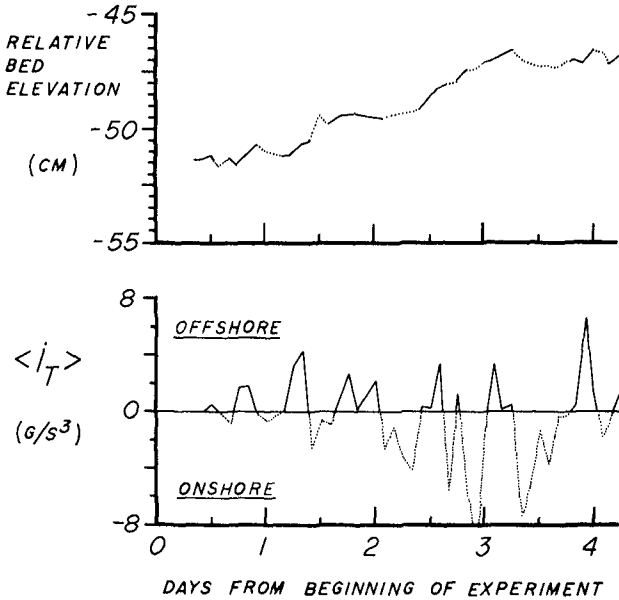


Figure 5. Burst-averaged relative bed elevation, expressed as cm below the fixed elevation of the DSA transducer, and predicted total-load sediment flux at 8-m depth during the fairweather period. Both records are marked with a solid line when the predicted transport was offshore and with a dotted line when the predicted transport was onshore.

	PREDICTED TRANSPORT DIRECTION	
	Offshore	Onshore
	-----	-----
	+0.00388	-0.00218
	+0.00221	-0.00267
$\frac{dz}{dt}$	+0.00083	+0.00094
(cm/min)	+0.00017	+0.00154
	+0.00375	-0.00065
	+0.00204	-0.00267
	+0.00171	-0.00592
	+0.00317	
	-----	-----

Table 1. Observed time-rate-of-change of relative bed elevation at 8-m depth during fairweather, calculated over consecutive bursts in which predicted transport direction (onshore or offshore) remained constant.

observed bed response at the 8-m depth site: times of predicted offshore transport (the solid line in the lower panel) correspond to times of relatively rapid accretion (the solid line in the upper panel), and times of predicted onshore transport (dotted line in lower panel) correspond to erosion or relatively slower accretion (dotted line in upper panel), with only a couple of exceptions. There were seven separate periods when the predicted total sediment flux was onshore over consecutive bursts and eight separate periods when the predicted total sediment flux was offshore over consecutive bursts. The change in burst-averaged relative bed elevation over each of these periods was calculated and these values are shown in Table 1, grouped by predicted transport direction. The observed rates of change in relative bed elevation (Table 1 and Figure 5) confirm the link between predictions and observations: there is a strong correlation between predicted offshore transport and observed accretion, and between predicted onshore transport and observed erosion at the 8-m depth site. Equation (1) is therefore a useful predictor, at least qualitatively, of the bed response to competent fairweather flow at this 8-m depth site. A more quantitative verification, comparing observed and predicted sedimentation rates, for example, would require a detailed analysis of the sediment-flux divergence associated with the competent flow.

The correlation between mean flow, which was driving transport direction at 8-m depth, and bed response highlights a fundamental difficulty with equation (1). Although the vertical variation of the mean flow in a combined-flow boundary layer is known theoretically (e.g. Grant and Madsen, 1979), it is not at all clear at which elevation the mean flow must be measured for use in the transport model. This problem precludes any further analysis of transport rates here, even though transport directions predicted on the basis of the velocity measured at $z = 20$ cm appear justified. Green (1987) circumvented this difficulty by using a traction model of transport, in which the combined-flow bed shear stress drives the sediment flux. The importance of the mean flow also emphasizes a potential deficiency of the electromagnetic current meter, which is presently in widespread use. Although Bowen and Doering (1984) found that the measurement of pure-wave skewness using electromagnetic current meters was rather more consistent than expected, and indeed the skewness measurements reported herein appear to be sensible, recent detailed laboratory tests by Aubrey and Trowbridge (1985) have shown that it may be difficult to obtain accurate estimates of the mean flow using these instruments.

Storm

The DSA data obtained during the storm were significantly noisier than the fairweather data; high concentrations of suspended sediment in the line-of-sight of the transducer caused premature echoes and signal scattering that occasionally resulted in complete loss of

echo detection (Green and Boon, 1988). Even after removal of the primary spikes, significant noise remained in the record, which may have biased the estimates of burst-averaged relative bed elevation. Therefore, only gross trends can be examined with confidence. The major features of the storm record were: a negligible change in bed level in response to the initial impulse of the wind; -5 cm of bed scour during the mid-phase of the storm; and -15 cm of rapid accretion during the waning phase of the event (Figure 6).

A significant feature of the storm record is the change from erosion to rapid accretion of the bed that occurred approximately two days after the onset of the storm. This corresponded to a sudden increase in the magnitude of the predicted total-load transport (Figure 6), however there was no fundamental change in the sedimentation rate corresponding to the predicted change in transport direction shortly afterwards. The initiation of accretion was also roughly coincident with the beginning of the period of wave organization following the initial phase of the storm, as reflected by the wave skewness (Figure 6); furthermore, as the wave-orbital velocities became increasingly skewed, the accretion rate increased, culminating in a maximum in both towards the end of the experiment.

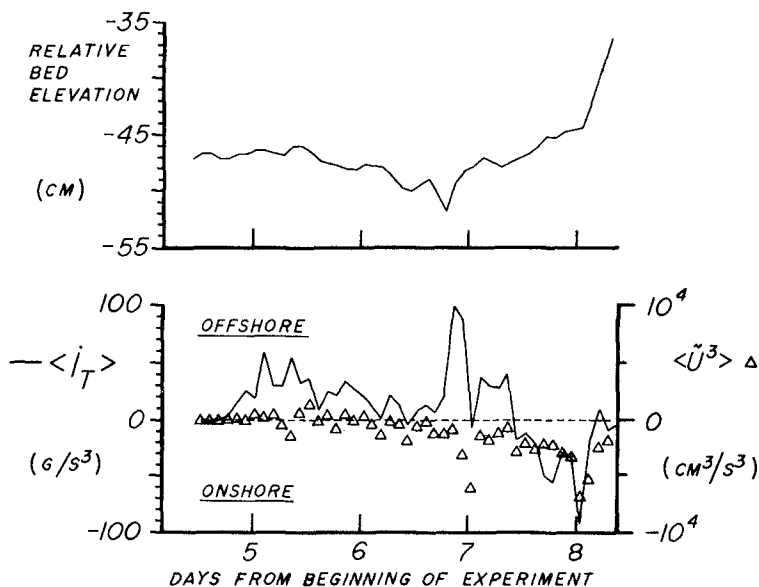


Figure 6. Burst-averaged relative bed elevation, expressed as cm below the fixed elevation of the transducer, predicted total-load sediment flux, and wave-orbital velocity skewness at 8-m depth during the storm.

Storm sedimentation thus differed fundamentally from fairweather sedimentation, and equation (1) failed as an indicator of bed response under the storm conditions. This test, however, does not necessarily constitute invalidation of the transport model; it may be that there is a complex relationship between sedimentation (measured by the sonar altimeter) and sediment transport (predicted by equation 1) during high-energy conditions. For example, it appeared that the bed responds primarily to the oscillatory component of the combined flow. Another possibility is that the measured accretion reflects the migration of a large-scale bedform under the sensor; Wright et al. (1986) argued that the rapidity of the accretion was suggestive of a pulse-like migration of a sediment front or large-scale bedform over the installation site, and showed side-scan sonar imagery to support that hypothesis.

Conclusions

During fairweather at the 8-m depth site, the predicted cross-shore burst-averaged bedload and suspended-load fluxes were approximately equal in magnitude and, since the near-bed velocity was both highly skewed and not very energetic, the predicted downslope flux of sediment under the influence of gravity was relatively insignificant. The mean flow dominated the asymmetry of the observed velocity distributions, indicating that transport direction was controlled by the tidal mean flow rather than by the wave-orbital velocity asymmetry.

There was a strong correlation between observed sedimentation rates at 8-m depth during low-energy conditions and net burst-averaged sediment transport predicted by Bailard's (1981) combined-flow transport model. This correlation constitutes qualitative verification of the transport predictions. Since it was the mean flow at 20 cm above the bed that dominated the significant terms in the transport equation, fundamental difficulties in the transport equation and potential instrument deficiencies cannot be ignored.

Predicted net transport during the storm was directed offshore under the dominant control of the wind-driven mean flow, except towards the end of the storm when predicted net transport was turned onshore by highly-skewed wave-orbital velocities. Unlike fairweather transport, suspended load constituted more than 75% of the total load during the more energetic storm flow. There appeared to be a correlation between the skewness of the oscillatory component of the total flow and sedimentation during the storm, even though the mean flow again dominated predicted net transport. While not invalidating the transport predictions, since the exact relationship between sedimentation and sediment transport is unknown, the oscillatory flow may control storm sedimentation, at least during certain phases of the storm.

Acknowledgements

This study was supported by the Virginia Institute of Marine Science and the National Science Foundation, Grant No. OCE-8610635. We thank Bob Gammisch for expert assistance in the field, and Captain Durand Ward of the R/V Captain John Smith. Thanks are also due to Curt Mason and Bill Birkemeier of the U.S. Army Corps of Engineers' Field Research Facility. Contribution No. 1459 from the Virginia Institute of Marine Science.

References

- Aubrey, D.G. and Trowbridge, J.H., 1985. Kinematic and dynamic estimates from electromagnetic current meter data. *J. Geophys. Res.*, 90: 9137-9146.
- Bagnold, R.A., 1963. Mechanics of marine sedimentation. In: M.N. Hill (Editor), *The Sea*, Vol. 3. Wiley-Interscience, New York, pp. 507-528.
- Bailard, J.A., 1981. An energetics total load sediment transport model for a plane sloping beach. *J. Geophys. Res.*, 86: 10,938-10,954.
- Bowen, A.J., 1980. Simple models of nearshore sedimentation; beach profiles and longshore bars. In: S.B. McCann (Editor), *The Coastline of Canada*. Paper 80-10, *Geol. Surv. of Canada*. p. 1-11.
- Bowen, A.J. and Doering, J.C., 1984. Nearshore sediment transport: estimates from detailed measurements of the nearshore velocity field. *Proc. 19th Int. Coastal Eng. Conf.*, Houston, A.S.C.E., pp. 1703-1714.
- Grant, W.D. and Madsen, O.S., 1979. Combined wave and current interaction with a rough bottom. *J. Geophys. Res.*, 84: 1779-1808
- Green, M.O., 1987. Low-energy bedload transport by combined wave and current flow on a southern Mid-Atlantic Bight shoreface. Unpublished Ph.D. Dissertation, College of William and Mary, Williamsburg, Virginia, 160 pp.
- Green, M.O. and Boon, J.D., 1988. Response characteristics of a short-range, high-resolution, digital sonar altimeter. *Mar. Geol.*, in press.
- Guza, R.T. and Thornton, E.B., 1985. Velocity moments in nearshore. *Proc. A.S.C.E.*, *J. Waterway, Port, Coastal and Ocean Eng.*, 111: 235-256.
- Mason, C., Birkemeier, W.A. and Howd, P.A., 1987. Overview of DUCK85 nearshore processes experiment. *Coastal Sediments '87*, New Orleans, pp. 818-833.
- Sternberg, R.W., 1972. Predicting initial motion and bedload transport of sediment particles in the shallow-marine environment. In: D.J.P. Swift, D.B. Duane and O.H. Pilkey (Editors), *Shelf Sediment Transport: Process and Pattern*. Dowden, Hutchinson and Ross, Stroudsburg, Pennsylvania, pp. 6-82.
- Wright, L.D., Boon, J.D., III, Green, M.O. and List, J.H., 1986. Response of the mid shoreface of the southern mid-Atlantic Bight to a "northeaster". *Geo-Marine Letters*, 6: 153-160.